AUTOMATIC GLACIER SURFACE ANALYSIS FROM AIRBORNE LASER SCANNING

M.P. Kodde [a], N. Pfeifer [b], B.G.H. Gorte[c], T. Geist[d], B. Höfle[e]

a. Fugro-Inpark, Dillenburgsingel 69, 2263 HW Leidschendam, The Netherlands - m.kodde@fugro-inpark.nl
b. Institute of Photogrammetry and Remote Sensing, Vienna University of Technology - np@ipf.tuwien.ac.at
c. Delft University of Technology, Kluyverweg 1, 2629 HS Delft, The Netherlands b.g.h.gorte@tudelft.nl
d. FFG – Austrian Research Promotion Agency, Sensengasse 1, 1090 Vienna, Austria – thomas.geist@ffg.at
e. Institute of Geography, University of Innsbruck, Innrain 52, 6020 Innsbruck, Austria – bernhard.hoefle@uibk.ac.at

KEY WORDS: Airborne Laser Scanning, DEM, Glacier, Crevasses, Mathematical Morphology

ABSTRACT:

Glaciers are interesting phenomena to scientists, mountaineers and tourists. Glaciers have a great impact on the local economy, power generation and water supply. Furthermore, the behaviour of glaciers is influenced by climate variations, such as changes in temperature. Monitoring glaciers can therefore give valuable insight to glaciologists. Two aspects of glaciers that can be monitored are the delineation of a glacier and the crevasses within a glacier. In this paper it is presented how these two aspects can be detected automatically from Airborne Laser Scanning (ALS) data.
The delineation of a glacier can be derived from ALS data by setting up a classification of the elevation model into the classes *glacier* and *non-glacier surface*. The smoothness, which is calculated from the ALS data, is used as classification criterion. Crevasses within the glacier can be detected by assuming that they are deviations from a regular glacier surface without any crevasses. Such a surface can be calculated with techniques from Mathematical Morphology. Given the assumption that crevasses have a V-like shape, the bottom of the crevasse and the two edges can be reconstructed from the point data. ALS data that was acquired at the Hintereisferner in Tyrol, Austria was used for testing the algorithms. Both the delineation of the glacier and the detection of crevasses give good results in the presented approach. However, the delineation of the glacier might fail if many crevasses cause exceptions to the smoothness criterion. Crevasses are sometimes not detected due to snow bridges. The quality of the reconstruction of crevasses is hard to assess due to the lack of reference data at the test location. Data acquisition with a higher point density and the acquisition of reference data for crevasses with Terrestrial Laser Scanning are recommended to independently check the result.

1. INTRODUCTION

Glaciers are sensitive indicators for climate change processes and have a significant impact on water supply in some regions. Several authors have shown that there is a relation between melting of glaciers and several climatologic parameters, including temperature (Oerlemans, 1994). Glaciers are also of great economic interest on a regional scale. In some regions hydro-power generation, drinking water supply and tourism rely heavily on the existence of glaciers. For these regions, a good understanding and monitoring of glaciers is of vital interest.

For many decades, measurements of glacier length variations and glacier mass-balance have been made in differing ways with the purpose of monitoring the dynamics of the glacier. This was done by means of terrestrial measurements, or by using aerial based data such as photogrammetry. In the European Union funded research project "Operational Monitoring System for European Glacial Areas (OMEGA)", several methods for glacier monitoring were explored, including Airborne Laser Scanning (Geist et al., 2005). Results from this project show the potential of ALS data for different applications in glacier research, thereby following up earlier attempts to utilise ALS on mountain glaciers (Baltsavias et al., 2001; Kennett and Eiken, 1997; Rees, 2005).

With the increasing availability of ALS data, automated approaches can be used to find specific properties of glaciers. Some of the information that can be extracted from the datasets is the extent of the glacier and the location of glacier crevasses. Crevasses are cracks in the upper surface of a glacier, formed by tension acting upon the brittle ice. They can be deep and thus dangerous for travellers on glaciers. Using ALS data to detect and reconstruct crevasses, will assist glaciologists to get more insight into ice dynamics.

Research in other fields of application has already shown that ALS data can be used with a high degree of automation. Objects such as buildings (Vosselman and Dijkman, 2001) and trees (Kraus and Pfeifer, 1998) can be detected automatically from the data. However, automated surface analysis has not yet been applied to glacier surfaces. Climate change sensitive objects, as glaciers are, will be monitored more intensively in future, necessitating automated approaches. In this paper methods for the automatic delineation of glacier areas will be presented and compared. Subsequently, a method for detecting and finally reconstructing crevasses will be presented.

2. DATA SETS

The methods presented were tested on ALS data that was acquired within the OMEGA project. One glacier in this project was the Hintereisferner in Tyrol, Austria. It is a typical valley glacier located in the Ötztal Alps. Up to now, 13 epochs of laser scanning data are available for the Hintereisferner. These datasets were acquired between October 2001 and September 2006 in different seasons of the glaciological year. The datasets acquired in the OMEGA project are documented in Geist and Stötter (2007). For the work in this paper, the data acquired on

August 12th 2003 (HEF9) and October 5th 2004 (HEF11) was used.

The acquisition of these two datasets was performed with the Optech ALTM 2050 and the Optech ALTM 1225 respectively. HEF9 had a mean flying height of 1150 m. For HEF11 the average flying height was 1000 m above the surface. The minimum slant range was 460 m, while the maximum was 1980 m. An average point distance of 0.8 m for HEF9 and 0.7 m for HEF11 was achieved. The vertical accuracy over a control area was σ = 0.095 m for HEF9 and σ = 0.075 m for HEF11. The full information of the points, i.e. values for first pulse, last pulse and intensity, is stored in a PostgreSQL database that can be connected to the GRASS GIS (Höfle et al., 2006). The other data sets were not yet added to the database at the time of writing. Additionally, the data was transformed to a 1 m resolution raster using a nearest neighbour interpolation method on the last pulse returns. The use of last pulse data increases the chance of getting points on the bottom of the crevasses. These resulting rasters form the input for the algorithms presented in the following sections.

3. GLACIER DELINEATION

For the detection and reconstruction of crevasses, it is required to limit the search area to the parts of a Digital Elevation Model (DEM) where a glacier can be found. This is done by automatically calculating the delineation of a glacier. Afterwards, the crevasse locations are detected and individual crevasses are reconstructed. The glacier delineation is not only of interest because it forms an important input to the crevasse detection algorithms, it is also an interesting result on itself. Delineations from repeated measurements can for instance be used to monitor the growth or decay of a glacier.

In the presented method it is assumed that the measurements are organised as a rasterised DEM. An example of such a DEM representing a glacier and the surrounding mountains is presented in Figure 1.

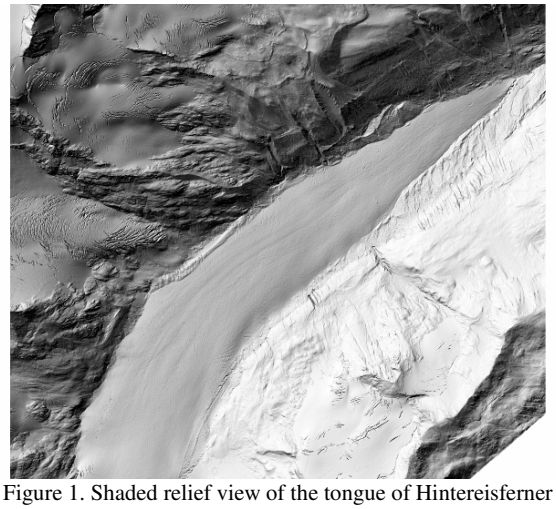

Figure 1. Shaded relief view of the tongue of Hintereisferner

Determining the delineation is essentially a classification of the pixels into the classes “glacier” and “non-glacier”. The process of classification is well-known from Remote Sensing where it normally involves the analysis of multispectral image data and the application of statistically based decision rules. This spectral data is now absent, but other criteria can be developed for the decision rules:

- Criterion 1: Smoothness
- Criterion 2: Connectivity
- Criterion 3: Hydrological constraints

Criterion 1 is based on the surface characteristics as they can be derived from the elevation data. The ice surface that makes up the glacier is much smoother than the surface of the surrounding bedrock. There are several ways to find the smooth areas in the DEM. One method is to calculate the variance of the best fitting plane in a certain region of cells. The size of this region depends on some surface properties and the grid sampling interval. By setting upper and lower boundaries to the variance, the smooth areas can be classified as glacier. The result of this calculation is a new map $\boldsymbol{\Sigma}$ which contains the variance of n surrounding points in each pixel $\boldsymbol{\Sigma}(r,c)$. The classification is now simply defined as applying a threshold t to this map:

$$\begin{cases} \mathbf{C}(r,c) = TRUE & for \;\; \boldsymbol{\Sigma}(r,c) < t \\ \mathbf{C}(r,c) = FALSE & for \;\; \boldsymbol{\Sigma}(r,c) \geq t \end{cases} \quad (1)$$

Alternatively, smoothness can be determined by segmenting the area first. For smooth areas we assume that the first derivative of the surface remains constant. Areas with constant first derivatives can be grouped in segments. If these segments are large enough, the surface that belongs to them can be considered smooth. In image processing, the first derivative of the data is usually called the gradient ∇z.

$$\nabla z = \left(\frac{\partial z}{\partial x} \quad \frac{\partial z}{\partial y} \right)^T \quad (2)$$

Numerically the gradient can be computed with the Sobel filter. Vosselman et. al. (2004) and Hoover et. al. (1996) treat different methods for segmentation in order to recognise structure in elevation models. One of the segmentation algorithms treated is the split-and-merge algorithm. For this work such a segmentation algorithm based on quad trees is used. The algorithm was designed by Gorte (1996) and has the advantage that it allows to segment on multiple bands simultaneously. In this case the x- and y-gradient images are the two bands on which the segmentation algorithm operates. After segmentation, we get a high number of different segments, which should now be classified in one of the classes ‘glacier’ and ‘non-glacier’. Only if a segment is relatively large, the surface can be called smooth. The problem of classifying glacier pixels can therefore be translated to the problem of selecting segments that are greater than a certain predefined area. By applying this classification method, the parts of the terrain that can be considered smooth are selected, resulting in the classification map $\mathbf{C}$.

Tests show that the results using the classification or the segmentation are practically equal. The size of differences observed fall within the grid resolution. In comparison to the variance based classification the segmentation method is computationally much more efficient because calculating the gradients requires less computational effort than fitting the planes through the data. However, when fitting the planes, slope

and aspect come as a side product, which may be interesting for other purposes.

Criterion 2 involves the connectivity of pixels classified as glaciers surface. In glaciology a glacier is considered as one large connected mass, mainly consisting of ice. Using connected component labelling, the result from the classification on criterion 1 can be improved by applying the connectivity constraint.

The last criterion that is used to improve the delineation is related to the hydrological properties of glaciers. Given some exceptional circumstances, glaciers generally flow downwards. Consequently, the notion of a catchment area also applies to glaciers. A catchment is the area in which all water, ice or snow flows to the same single outlet. Any pixel classified as glacier should therefore lie within the catchment area of the glacier. This criterion is therefore used to limit the extent of the glacier. Most GIS software contains methods to calculate such a catchment boundary from a DEM.

In the end, the results of the three criterions can be combined to get the final delineation of the glacier. A further improvement of the glacier surface could be obtained by using intensity based segmentation. (Höfle et al., 2007)

4. CREVASSE DETECTION

4.1 Detection using Mathematical Morphology

In order to extract crevasses from a DEM and visualise their locations, we try to create a flat surface with only non-zero values at crevasse locations. The part that has to be removed from the original DEM is the glacier surface as well as the elevation of underlying bedrock. The physical meaning of these elevations would be a glacier in which no crevasses were formed. In order to obtain this surface some techniques from mathematical morphology are used.

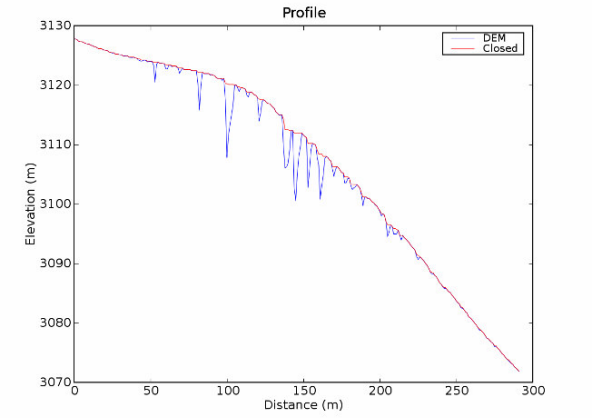

Figure 2. Cross section of a glacier with the result of the closing operation

Mathematical morphology is the theory of the analysis of spatial structures in data sets. It works like a convolution, but uses decision operators instead of multiplication. A morphological filter is used to detect or modify structural elements in the image, i.e. the morphology of the terrain. Provided that the structuring element is larger than the width of the crevasse, the closing filter will close all crevasses, effectively removing them from the glacier surface. Figure 2 shows a profile of the glacier after performing the closing filter. Having generated this surface of a glacier without crevasses, the closed surface is subtracted from the original data, an operation that is known as Black Top Hat. Applied to the DEM, the resulting dataset will be zero over the whole terrain, except for the locations with a crevasse. Given the DEM $\mathbf{H}$, the Black Top Hat operation is now defined as:

$$\mathbf{H}_{\mathbf{crev}} = BTH\left(\mathbf{H}\right) = \phi\left(\mathbf{H}\right) - \mathbf{H} \qquad (3)$$

where $\phi\left(\mathbf{H}\right)$ represents the closing operation over the DEM. Because the filter closes the crevasses horizontally, the filtered surface is not exactly a surface without crevasses because this will be a sloped surface. This problem was solved by detrending the data first, so that the horizontal closing gives the correct result. This detrending of the DEM, i.e. removing the large scale relief features, can for instance be done by top-hat filtering with a very large window size.

4.2 Setting the structuring element size

After detrending, the crevasse-less glacier surface should be perfectly flat. This means that a flat structuring element can be used, i.e. a structuring element where the shape is defined by the value '1'. The size of the structuring element can be seen as a definition of how long (or how far) the morphology in the structuring element holds. Often, the correct filter size is hard to determine. In this work a novel method is explored to formalise the structuring element size using a variogram of the terrain. A variogram is a measure of the variance between data as a function of distance. The theoretical variogram is defined as:

$$\gamma\left(d\right) = \tfrac{1}{2} E\left\{\left[\underline{h}(p+d) - \underline{h}(p)\right]^2\right\} \qquad (4)$$

Where p is a point in the DEM, $\underline{h}\left(p\right)$ the height of that point and d the distance from that point. Figure 3 gives the theoretical variogram based on the Gaussian model for a selected small part of the glacier surface. For comparison, the scatter- and experimental variograms are displayed as well. The values found after fitting the Gaussian model were a range of R = 369 m and a sill σ^2 = 1.3 m^2.

From the theoretical variogram, measures of variance in the terrain can be related to the size of the structuring element. For instance, field measurements with a Terrestrial Laser Scanner on the Hintereisferner in the summer of 2006 showed that a variance of 0.06 m^2 (0.25 m standard deviation) can be expected within a small area on the glacier. The variogram relates this to a structuring element size of 10 m in diameter.

The shape of the structuring element depends on the anisotropy of the glacier. The amount of anisotropy can be determined by calculating a directional variogram. On a perfect isotropic surface, the variogram will be equal in all directions, yielding a disk shaped structuring element. On anisotropic surfaces, the directional variogram is used to form an ellipse-shaped structuring element. In this study only isotropic structuring elements were applied.

Implementing the variogram method in the detection software, means that an operator can select the amount of variance he or she assumes on a glacier surface without crevasses. The program then takes care of setting the right parameters for the filter.

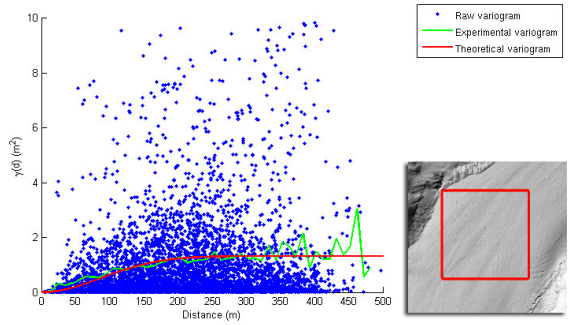

Figure 3. The fitted variogram of a part of the glacier surface

5. CREVASSE RECONSTRUCTION

Whilst the delineation of the glacier and the detection of crevasses were solely performed on height measurements that were interpolated to a grid, the reconstruction of crevasses will be done on the unprocessed point data. The point data for a crevasse is selected using the crevasse locations found in the previous step. A problem with reconstructing crevasses is the relative low point density of 1 point per square meter. This density is low compared to the average crevasse width of a few metres, which requires us to make some assumptions in the reconstruction.

If it is assumed that crevasses have a regular V-like shape, it is possible to parameterise this shape into a geometrical object. A simple parameterisation would consist of parameters for depth, width and length. Unfortunately, crevasses are not that simple: they are usually bended and do not have a constant depth. Describing this in parameters is infeasible; therefore the crevasses will be reconstructed using a boundary representation. Taking the V-shape as a basis, we can build a crevasse with three lines: a bottom line and two upper surface edges. These three lines are connected at the beginning and the end of the crevasse.

The bottom line is the first line to extract, using a process that consisting of two steps. The first step constitutes the determination of the horizontal position of the line. In the second step, z-coordinates are calculated for this line. It is unlikely that there are any laser points that lie exactly on the bottom line of the crevasse. The location of the bottom line must therefore be derived from the surrounding pixels. It can be assumed that the horizontal position of the bottom line lies in the middle of the crevasse. The program selects the lowest 25 percent of the points in the crevasses and calculates the centre by fitting a spline though these points. After fitting, the program removes points with a large residual and tries to fit the line again, giving an improved position.

The result of fitting the polynomial can further be improved by giving weights to the points used in the adjustment. Points with a large depth are given a higher weight in the adjustments, while points near the surface get a lower weight. We call the estimated polynomial coefficients $\underline{\hat{x}}$, the weight matrix W and the design matrix A. If the stochastic x an y coordinates are combined in the random vector $\underline{y}$, the Least Squares Adjustment is given by: $\underline{\hat{x}} = \left(A^* W A\right)^{-1} A^* W \underline{y}$. Then the weights are derived as:

$$w_{ii} = \left(\frac{h_i - h_{\min}}{h_{\max} - h_{\min}} \right)^2 \quad i = 0,1,\ldots n-1 \qquad (5)$$

Taking these weights in an iterative approach, gives the horizontal position of the bottom line. The next step is to assign elevations to this line. This can be done by taking the convex hull over the lowest 25% of the points, like depicted in Figure 4. However, the reconstructed depth will be highly uncertain, as there might be snow in the crevasse, obstructing the bottom from the laser beam. The reliability will also depend on the sampling interval.

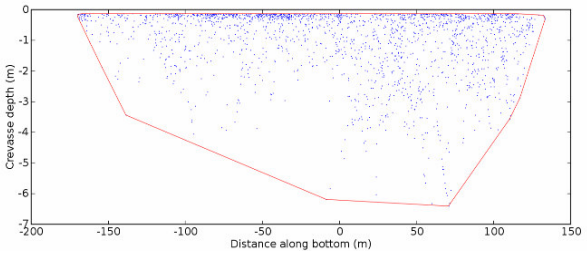

Figure 4. Laser points in a crevasse. The proposed bottom line is drawn in red

The remaining step comprises the modelling of the edge of the crevasse, the line where the glacier stops and the crevasse starts. For finding the edge, profiles of points were generated perpendicular to the bottom line that was found before. For the selected test crevasse, 152 profiles were made with an in-between spacing of 2 meters. In each of these profiles, the locations of the left and right edge were searched independently.

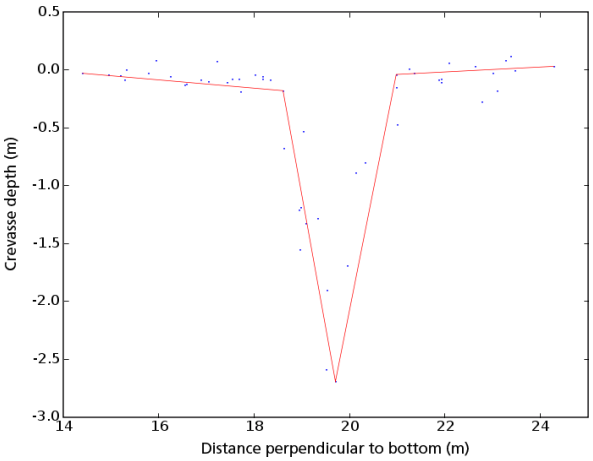

Figure 5. Cross section of a crevasse with generalisation result

To find the crevasse edges in the profiles, an algorithm was developed, based on the Douglas-Peucker line simplification algorithm. This algorithm reduces the number of points until

only the most important points for the profile shape remain. These points are the start and end points of the profile, the two edges and the bottom. Figure 5 shows one of these profiles with the laser points (in blue) and the profile (in red) after applying the simplification algorithm. When all edge points are found in the individual profiles, a spline fitting algorithm is used to connect and smooth the points for the final edge lines.

The points that are found on the bottom line and the two edge lines can be used for generating a Triangulated Irregular Network (TIN). From the TIN, it is possible to calculate values for the volume and shape of the crevasse.

6. RESULTS

The methods and algorithms described in the previous sections were implemented as a part of the LiSA toolbox, which is maintained by the University of Innsbruck. The program uses GRASS GIS (GRASS Development Team, 2006) for data storage and graphical output. The methods were tested on two epochs of the Hintereisferner ALS data.

6.1 Glacier delineation

The delineation of the Hintereisferner was determined by calculating the variance for all pixels in the DEM using the best fitting planes method that was presented in section 3. The window size used was 11 by 11 pixels with a resolution of 1 m per pixel. The surface variance that we find in the DEM is a combination of the measurement precision and the variation in the terrain: $\sigma^2_{DEM} = \sigma^2_{ALS} + \sigma^2_{SURFACE}$.

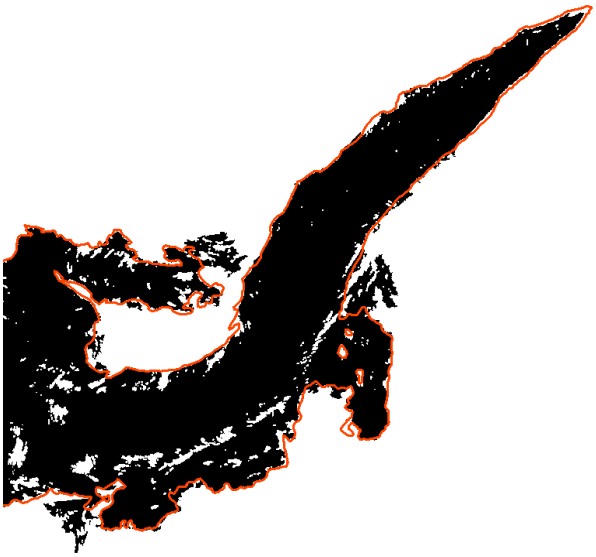

Figure 6. Area classified as glacier for the Hintereisferner DEM (black) and the manual delineation (red)

If we only look to pixels on the glacier surface of the Hintereisferner, variance values up to 0.06 m^2 were found, which implies a standard deviation of 0.25 m. This is approximately twice the specified laser scanning system variance σ^2_{ALS}. This variance was used as the classification threshold t for assigning pixels to the classes "glacier" and "non-glacier". The boundary of the "glacier" class will give the delineation of the glacier. This delineation was further improved by smoothing it with a binary 3x3 morphological closing filter and intersecting it with the hydrological boundaries. Figure 6 shows the resulting area that has been classified as Hintereisferner.

The calculated delineation is a good representation of the real glacier extent. Only at some crevasse locations errors in the delineation occur. This is because the gaps at crevasse locations cause a higher surface variance, which is above the specified threshold value. Fortunately, these errors can easily be resolved, although they require manual intervention. One way to assess the quality of the delineation is to compare it with a delineation that was acquired manually by an experienced glaciologist. Comparing the computed delineation with the manual delineation gives an overall kappa value of 0.82. A comparison of the classified pixels in the manually made reference map and the classification result is given in Table 1 and Table 2.

		Reference Map	
	Classes	No Glacier	Glacier
Classification	No Glacier	19665553	1122511
	Glacier	611266	5639118

Table 1. Number of pixels assigned to each class.

Classes	Commission	Omission	Estimated $\hat{k}$
No Glacier	5.88 %	3.29 %	0.780
Glacier	7.78 %	16.60 %	0.867

Table 2. Confusion matrix of glacier classification.

6.2 Crevasse detection

In the previous sections a method was presented for detecting crevasses in a glacier using mathematical morphology. Within the boundaries formed by the glacier delineation, the crevasse detection algorithm can now be applied. The crevasse detection was applied to two laser scanning epochs of the Hintereisferner dataset, taken in different seasons. Figure 7 shows the detected crevasse locations on a part of the glacier in the summer season. In this figure only crevasses deeper than 0.4 meters are shown.

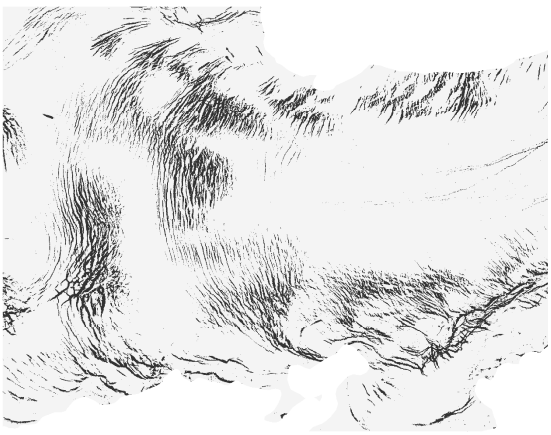

Figure 7. Detected crevasse locations.

From the variogram analysis it showed that a structuring element size of 10 m was most optimal for detecting the crevasses. In order to assess the quality of the crevasse detection one should consider the geometrical accuracy as well as the classification accuracy, i.e. how many crevasses are classified as glacier surface and how much glacier surface is classified as

crevasse? In the absence of any reference data, it was not possible to assess the quality of the results. However, by overlaying the detected crevasses over an orthophoto of the same time, a visual inspection was made. The visual inspection revealed that there were not crevasses found on the orthophoto that were missing in the automatic detection. The crevasse detection obviously gives wrong results when the crevasses are filled with snow or covered by snow bridges.

7. CONCLUSION

With the methods presented in this paper, it is shown that Airborne Laser Scanning is an accurate and reliable tool for monitoring glaciers and crevasses. Glaciers can be delineated from ALS data at an accuracy of the pixel size. The delineation used smoothness as well as some other classification criteria to find the outer boundaries of the glacier. This method takes the implicit assumption that glaciers can be recognised by a smooth surface. At crevasse locations this assumption doesn't hold and therefore the method still needs human supervision. It is also possible to detect the location of crevasses from ALS data, provided that the glacier surface is not covered by snow so the crevasses are visible for the laser beam. Additionally the crevasse should be wider than the pixel resolution. It also requires the glacier delineation as input.

Reconstructing crevasses is difficult because of the low sampling interval. The number of data points in the given dataset was too little to reliably reconstruct the crevasse without making assumptions. Additionally, specific situations, such as snow bridges, make the reconstruction even more unreliable. However, individually reconstructed crevasses do give a good indication of quantitative measures such as the volume and length of crevasses. Additionally, the area of the crevasses can be measured, even without reconstruction of its depth. For reconstructing crevasses, it is assumed that they are not covered by snow and have a V-like shape. In reality, some crevasses can have an A-shape, which can therefore not be reconstructed.

The results of the developed program can be used for the applications identified in the introduction of this paper. Interest has also been shown in some other fields, such as cartography of glaciers. To increase automation, studies on other (types of) glaciers and with data acquired in different seasons are necessary.

ACKNOWLEDGEMENTS

The authors would like to acknowledge alpS - Centre for Natural Hazard Management in Innsbruck, Austria for their support.

REFERENCES

Baltsavias, E.P., Favey, E., Bauder, A., Bosch, H., Pateraki, M., 2001. Digital Surface Modelling by Airborne Laser Scanning and Digital Photogrammetry for Glacier Monitoring. *The Photogrammetric Record*, Vol. 17, Part 98, pp 243-273.

Geist, T., Elvehøy, H., Jackson, M., Stötter, J., 2005. Investigations on intra-annual elevation changes using multitemporal airborne laser scanning data – case study Engabreen, Norway. *Annals of Glaciology*, Vol. 42, pp 195-201.

Geist, T., Stötter, J., 2007. Documentation of glacier surface elevation change with multi-temporal airborne laser scanner data – case study: Hintereisferner and Kesselwandferner, Tyrol, Austria. *Zeitschrift für Gletscherkunde und Glazialgeologie*, Vol. 40.

Gorte, B.G.H., 1996. Multi-spectral quadtree based image segmentation. *International Archives of Photogrammetry and Remote Sensing*, Vol. 31, pp 251-256.

GRASS Development Team, 2006. Geographic Resources Analysis Support System (GRASS) Software. ITC-irst, Trento, Italy.

Höfle, B., Geist, T., Rutzinger, M., Pfeifer, N., 2007. Glacier Surface Segmentation using Airborne Laser Scanning Point Cloud and Intensity Data, ISPRS Workshop on Laser Scanning 2007, Espoo, Finland.

Höfle, B., Rutzinger, M., Geist, T., Stötter, J., 2006. Using airborne laser scanning data in urban data management - set up of a flexible information system with open source components, Proceedings of UDMS 2006: 25th Urban Data Management Symposium, Aalborg, Denmark, pp. 7.11-7.23.

Hoover, A., Jean-Baptiste, G., Jiang, X., Flynn, P.J., Bunke, H., Goldgof, D.B., Bowyer, K., Eggert, D.W., Fitzgibbon, A., Fisher, R.B., 1996. An Experimental Comparison of Range Image Segmentation Algorithms. *IEEE Trans. Pattern Anal. Mach. Intell.*, Vol. 18, Part 7, pp 673-689.

Kennett, M., Eiken, T., 1997. Airborne measurement of glacier surface elevation by scanning laser altimeter. *Annals of Glaciology*, Vol. 24, pp 293-296.

Kraus, K., Pfeifer, N., 1998. Determination of terrain models in wooded areas with airborne laser scanner data. *ISPRS Journal of Photogrammetry & Remote Sensing*, Vol. 53, pp 193-203.

Oerlemans, J., 1994. Quantifying Global Warming from the Retreat of Glaciers. *Science*, Vol. 264, pp 263-245.

Rees, W.G., 2005. Remote Sensing of Snow and Ice. Taylor & Francis.

Vosselman, G., Dijkman, S., 2001. 3D Building Model Reconstruction from Point Clouds and Ground Plans. *International Archives of Photogrammetry, Remote Sensing and Spatial Information Sciences*, Vol. XXXIV, Part 3/W4, pp 37-44.

Vosselman, G., Gorte, B.G.H., Sithole, G., Rabbani, T., 2004. Recognising Structure in Laser Scanner Point Clouds. *The International Archives of the Photogrammetry, Remote Sensing and Spatial Information Sciences*.